Improved Retrieval of Integrated Water Vapor from Water Vapor Radiometer Measurements Using Numerical Weather Prediction Models

STEVEN R. CHISWELL, STEVEN BUSINGER,* AND MICHAEL BEVIS*

Department of Marine, Earth and Atmospheric Sciences, North Carolina State University, Raleigh, North Carolina

FREDRICK SOLHEIM, CHRISTIAN ROCKEN, AND RANDOLPH WARE

University Navstar Consortium (UNAVCO), Boulder, Colorado

(Manuscript received 7 July 1993, in final form 15 February 1994)

ABSTRACT

Water vapor radiometer (WVR) retrieval algorithms require a priori information on atmospheric conditions along the line of sight of the radiometer in order to derive opacities from observed brightness temperatures. This paper's focus is the mean radiating temperature of the atmosphere (T_{mr}), which is utilized in these algorithms to relate WVR measurements to integrated water vapor. Current methods for specifying T_{mr} rely on the climatology of the WVR site—for example, a seasonal average—or information from nearby soundings to specify T_{mr}. However, values of T_{mr}, calculated from radiosonde data, not only vary according to site and season but also exhibit large fluctuations in response to local weather conditions. By utilizing output from numerical weather prediction (NWP) models, T_{mr} can be accurately prescribed for an arbitrary WVR site at a specific time. Temporal variations in local weather conditions can be resolved by NWP models on timescales shorter than standard radiosonde soundings.

Currently used methods for obtaining T_{mr} are reviewed. Values of T_{mr} obtained from current methods and this new approach are compared to those obtained from in situ radiosonde soundings. The improvement of the T_{mr} calculation using available model forecast data rather than climatological values yields a corresponding improvement of comparable magnitude in the retrieval of atmospheric opacity. Use of forecast model data relieves a WVR site of its dependency on local climatology or the necessity of a nearby sounding, allowing more accurate retrieval of observed conditions and increased flexibility in choosing site location. Furthermore, it is found that the calculation of precipitable water by means of atmospheric opacities does not require time-dependent tuning parameters when model data are used. These results were obtained using an archived subset of the full nested grid model output. The added horizontal and vertical resolution of operational data should further improve this approach.

1. Introduction

Ground-based water vapor radiometers (WVRs) provide measurements of integrated water vapor and integrated liquid water along lines of sight through earth's atmosphere (Resch 1984). These instruments are used by meteorologists for basic research into the distribution of water vapor (Hogg et al. 1981) and by geodesists (e.g., Elgered et al. 1991) and others to infer the "wet delays" affecting radio signals propagating through the atmosphere (Bevis et al. 1992). WVR retrieval algorithms involve parameters whose values must be specified a priori and that are known to vary according to site, season, and weather conditions. These parameters must be tuned to local conditions to optimize WVR performance. In this paper we focus on the most important of these parameters, the mean radiating temperature of the atmosphere (T_{mr}) and on an improved approach for estimating its value. Previous studies have employed a number of methods including calculating climatological values of T_{mr} based on the analysis of radiosonde data (Rocken et al. 1991); utilizing a linear correlation between T_{mr} and surface temperature, T_s (Wu 1979; Resch et al. 1985; Davis 1986); or using a method that combines climatological and surface measurement data (Askne and Nordius 1987; Robinson 1988). In this paper, we describe a new approach in which we exploit the prior information content of numerical weather prediction (NWP) models to estimate T_{mr}.

2. Precipitable water retrieval from water vapor radiometers

Water vapor radiometers have been used to estimate atmospheric precipitable water by relating the observed

* Current affiliation: Department of Oceanic and Earth Science Technology, University of Hawaii, Honolulu, Hawaii.

Corresponding author address: Steven Chiswell, Dept. of Marine, Earth and Atmospheric Sciences, Box 8208, Jordan Hall, North Carolina State University, Raleigh, NC 27695-8208.

antenna brightness temperature T_a, as measured by the radiometer, to atmospheric opacity, which can then be translated to integrated water vapor (or integrated liquid water content) and path delays. By introducing a mean radiating temperature T_{mr}, the opacity τ of the atmosphere at a given frequency can be expressed as

$$\tau = \ln\left(\frac{T_{mr} - T_{bg}}{T_{mr} - T_a}\right), \quad (1)$$

where T_{bg} is the contribution from background radiation sources (Davis 1986; Rocken 1988). The mean radiating temperature represents the effective radiating temperature of the atmosphere at a given frequency and is given by

$$T_{mr} \equiv \frac{1}{1 - e^{-\tau}} \int_{atm} T(s) e^{-\tau(s)} \alpha(s) ds, \quad (2)$$

where $\tau(s)$ is the optical depth and α is the absorption coefficient (Liou 1980; Davis 1986). The calculation of τ and α in (2) is provided in the appendix.

The value of T_{mr} varies according to site, season, and local weather conditions and must be computed or estimated from information not measured by the WVR instrument. Figure 1a depicts the time history of T_{mr} for 10 years at Greensboro, North Carolina, calculated from twice daily radiosonde soundings. The daily and seasonal variations in T_{mr} are distinguishable and dramatically demonstrate the ability for short-term fluctuations to be of comparable magnitude to that of the annual signal. Figure 1b presents a more detailed representation of T_{mr} over a two-month period where the effect of individual synoptic weather systems is evident. To provide useful estimates of precipitable water with time, an accurate time-dependent value of T_{mr} must be provided.

The retrieval of precipitable water (PW) from WVR measurements can be accomplished by utilizing the resultant measured opacities at two different frequencies to produce a linear combination of the form

$$PW = \alpha\tau_1 + \beta\tau_2 + \gamma, \quad (3)$$

where α, β, and γ are site-specific coefficients that can be tuned to local conditions in order to minimize the residual between the observed precipitable water and the calculated opacities (Rocken 1988). By computing values for τ_1, τ_2, and PW directly from sounding data for Greensboro, North Carolina, the values of the coefficients are found as $\alpha = 250.38$, $\beta = -144.04$, $\gamma = -0.31$ for frequencies $\nu_1 = 23.8$ GHz and $\nu_2 = 31.4$ GHz and PW in units of millimeters based on sounding data obtained from 1982 through 1992. Figure 2 shows the resultant precipitable water estimate obtained from (3) and the residual error based on the value of PW obtained directly from the soundings. A closer inspection of the residuals (Fig. 3) shows that the derived values of PW are generally within 0.6 mm of measured values, while the distribution of the errors is approximately normal. It is important to note that the additional term γ in (3) makes a small contribution to the resultant PW but arises due to errors in modeling the absorption coefficients as discussed in the appendix as well as instrumental uncertainties in radiosonde measurements.

Thus, if an acceptable estimate for T_{mr} is available, WVRs can produce an accurate measure of the integrated water vapor or the path delay of the atmosphere. From (1) we find that for an upward-looking WVR in which $T_{bg} \ll T_{mr}$, the error in opacity ($\delta\tau$) as measured by the radiometer can be expressed in terms of the errors in T_{mr} and T_a:

$$\frac{\delta\tau}{\tau} \approx \frac{\delta T_{mr}}{T_{mr}} + \frac{\delta T_a}{T_a}. \quad (4)$$

For a given WVR measurement with implied instrumental noise level, an improvement in the estimation of T_{mr} will lead to a corresponding improvement in the retrieval of opacity (Davis 1986). The current application of radiometers is also hindered due to the instrumental error introduced at low elevation angles and by precipitation. In general, the errors in T_{mr} become increasingly important as brightness temperature increases and the noise level of the radiometer decreases.

3. An evaluation of other methods for estimating T_{mr}

In the absence of observed values, WVR sites often employ climatological values of T_{mr}. Using (1) we can simulate a "perfect" WVR (i.e., one that possesses no instrumental errors or biases) by utilizing sounding data to calculate values of τ and T_{mr} directly and solving for the theoretical brightness temperature as seen by the WVR. Once the brightness temperature is known, we can determine the impact of the method in which T_{mr} is specified by reinserting estimates of T_{mr} into (1) and (3) to produce estimates of precipitable water. Finally these estimates of PW can be compared to the observed value in order to evaluate the method of specifying T_{mr}.

First we evaluate the use of a site annual mean T_{mr}. Figure 4 shows the residuals associated with this method: a sharply skewed distribution with prolonged periods of discrepancies greater than or equal to 2 mm. An investigation of the source of this skewed distribution reveals that it results from the application of an annually averaged T_{mr}, producing more extreme values in winter than in summer (Fig. 5). An improvement to this method is the use of a seasonally adjusted or monthly mean value for site. Figure 6 shows the residuals associated with using monthly mean values of T_{mr}. Although the range of the errors is dramatically decreased from the previous example, the residuals are still skewed. As seen in Fig. 1b, at a given midlatitude site T_{mr} can fluctuate by more than 5% with the passing of a frontal system. Therefore, setting T_{mr} to a seasonal

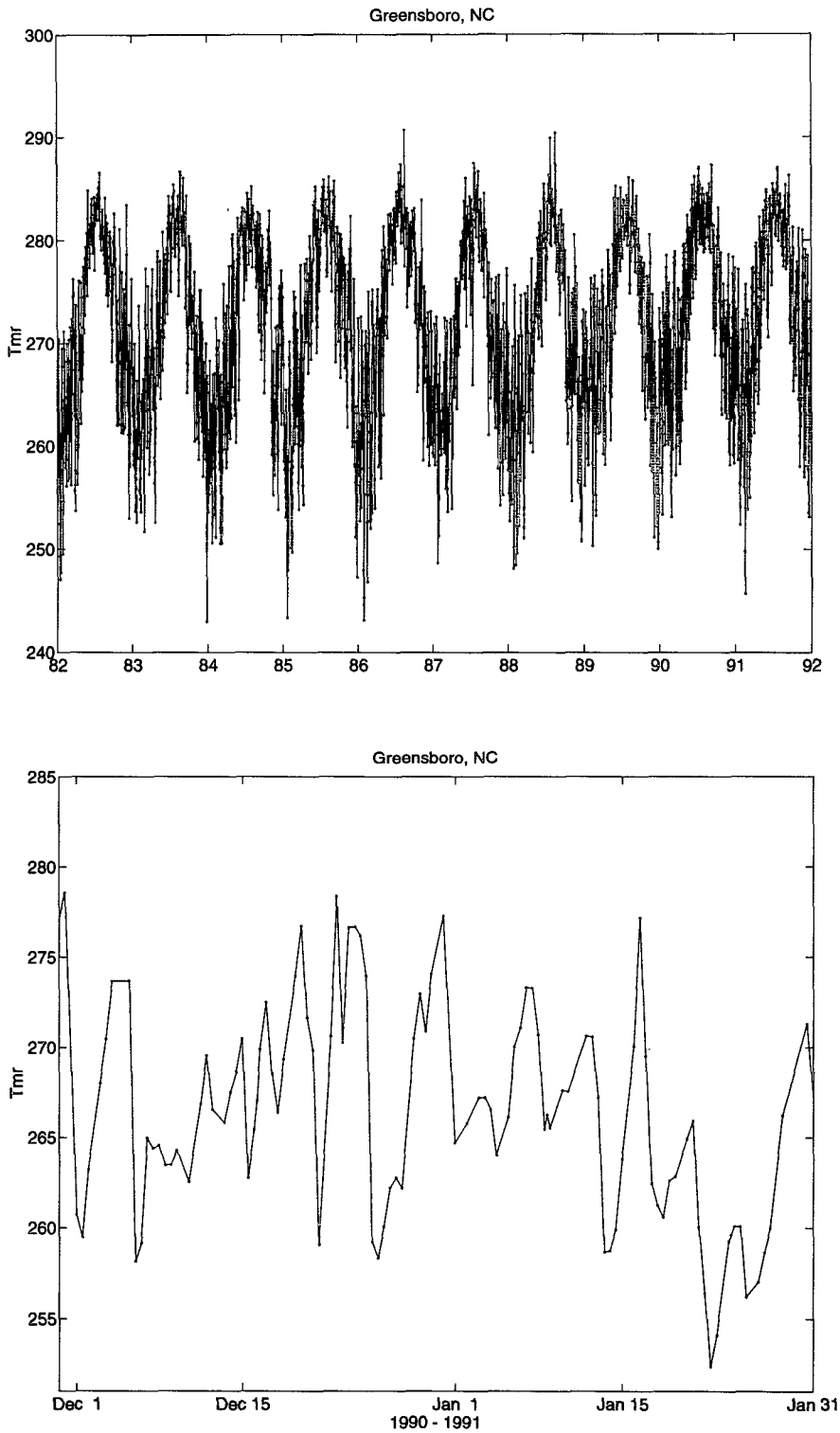

FIG. 1. (a) Time history of T_{mr} (31.4 GHz) for years 1982–91 at Greensboro, North Carolina, calculated from twice daily radiosonde soundings. (b) As in (a) except for 1 December 1990–31 January 1991.

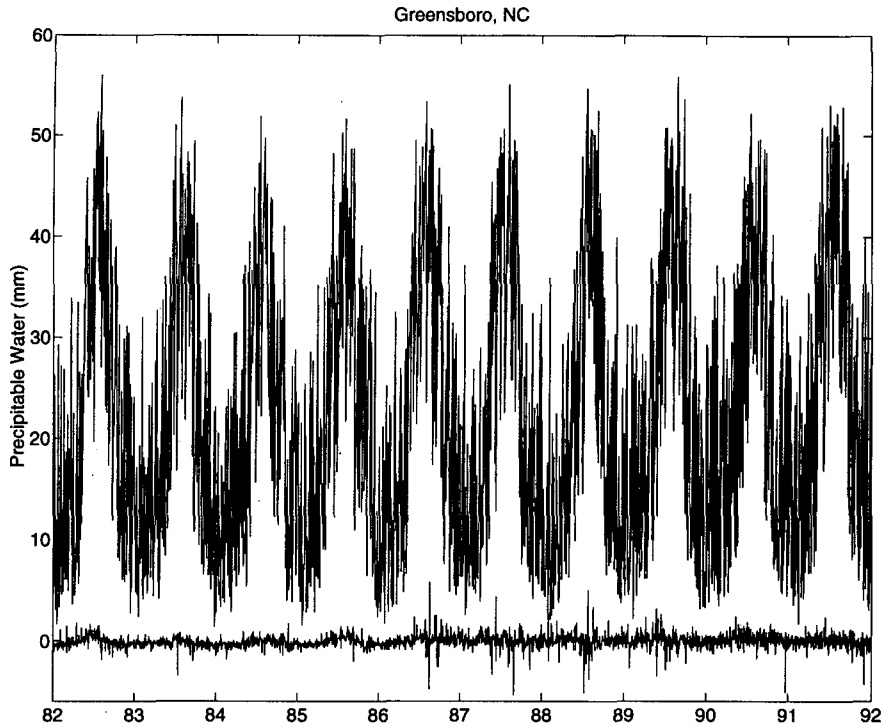

FIG. 2. Calculated precipitable water (top) and residuals (bottom) for years 1982–91 based on values of opacity and precipitable water calculated from Greensboro, North Carolina, sounding data.

average value can lead to unacceptably large errors in the value of opacity. As a result, retrieval algorithms that utilize seasonal values of T_{mr} must account for this time dependence by specifying a site- and season-dependent parameter for γ in (3) to compensate for the error (Rocken 1988). Thus, the inability to resolve the daily fluctuations in T_{mr} gives rise to an additional undetermined variable. Clearly the most desirable method for obtaining T_{mr} would be based on real-time in situ measurements.

In practice, the most basic of the methods for obtaining T_{mr} involve the use of a linear model based on surface temperature (Wu 1979; Resch et al. 1985; Davis 1986). Davis (1986) found that the seasonal error in T_{mr} for a single sounding station (e.g., Hilo, Hawaii, or Portland, Maine) could be tuned to the order of

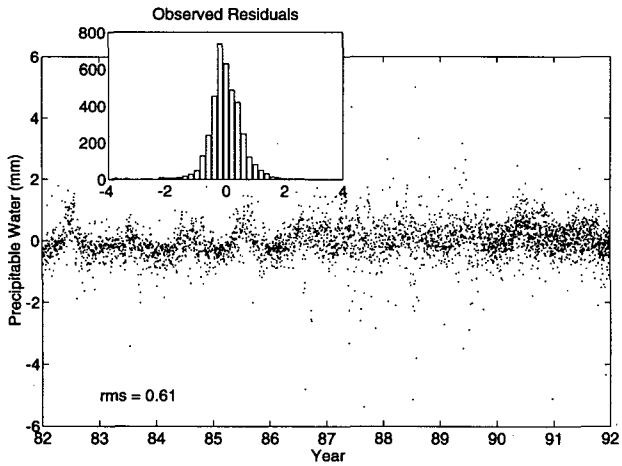

FIG. 3. Distribution of residuals from precipitable water prediction model.

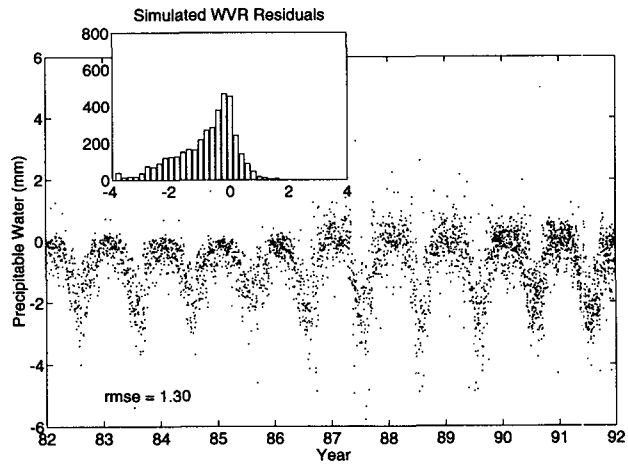

FIG. 4. Distribution of residuals calculated for a perfect WVR using annual mean T_{mr}.

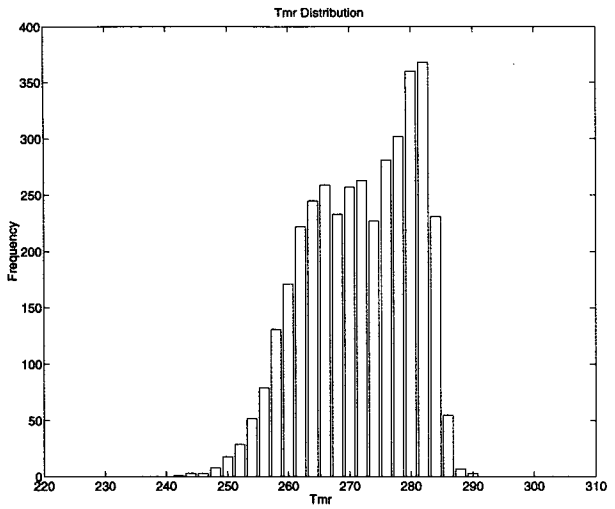

FIG. 5. Distribution of T_{mr} (31.4 GHz) derived from Greensboro, North Carolina (1982–92), sounding data.

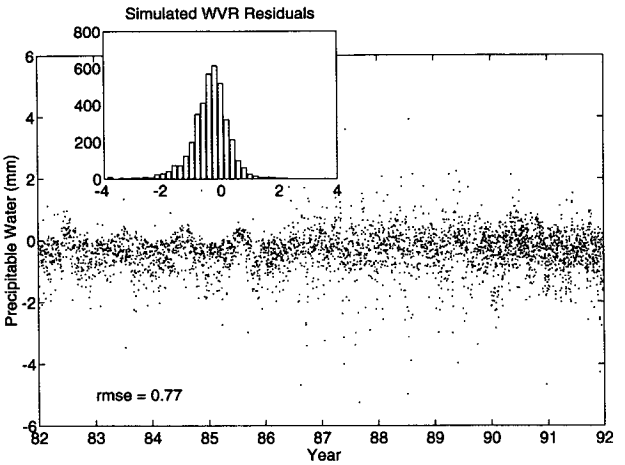

FIG. 6. Distribution of residuals calculated for a perfect WVR using monthly mean T_{mr}.

1%–2% using a linear model for surface temperature versus T_{mr} from radiosonde data; however, a large portion (up to 40%) of the soundings were not included. For comparison, we have computed T_{mr} for Greensboro, North Carolina, for all soundings taken from 1948 to 1991 (Fig. 7). Following the criterion given by Davis, 16 295 soundings were retained and 113 (0.7%) were rejected. The linear model of T_{mr} based on observed surface temperature for these times yields a root-mean-square error (rmse) of 4.57 K (1.7%). This result is in the range suggested by Davis. The major drawback of this method is the requirement of local soundings to derive the site-specific relationship. Temperature soundings that deviate greatly from climatology—for example, strong surface-based temperature inversions—are an important source of error inherent in this method. Additionally, cloud liquid water content may be important, and cannot be generally estimated from surface temperature.

The mean radiating temperature of the atmosphere has also been estimated using a profile algorithm such as that proposed by Robinson (1988), which uses surface measurements of temperature, pressure, and relative humidity; a standard profile of temperature (U.S. Standard Atmosphere Supplements 1966); and the climatological relative humidity at 3 km. In this study, the relative humidity was calculated from the initial analysis values of the European Centre for Medium-Range Weather Forecasts model taken from a 10-yr sample (1980–89), and soundings from the standard United States upper-air data network were collected. This method has the advantage over the method above in that it relieves a site of the dependency of a nearby sounding.

A nominal temperature profile of the atmosphere above the sounding location can be fitted from

$$T_{\text{nom}}(h) = T_{\text{US}}(h) + [T_{\text{surf}} - T_{\text{US}}(0)] \exp\left(-\frac{h}{H}\right), \tag{5}$$

where T_{US} is that taken from the U.S. standard atmosphere, T_{surf} is the observed surface temperature, and H is a scale height, with suggested value of 2 km. By using this formula, the station profile exponentially approaches that of the standard atmosphere, while allowing the profile to match the observed surface temperature. The corresponding nominal relative humidity profile is specified as a two-piece linear function joining the surface value with the observed value at 3 km and an assumed value of zero at 10 km. This derived profile is then similarly used to compute T_{mr} as outlined above.

By comparing values of T_{mr} obtained by the surface-based profile method at sounding locations against

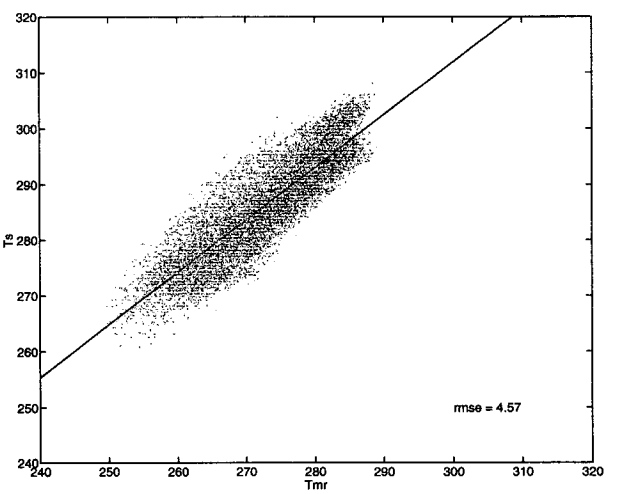

FIG. 7. Plot of T_{mr} (31.4 GHz) vs T_S for Greensboro, North Carolina, 1948–91.

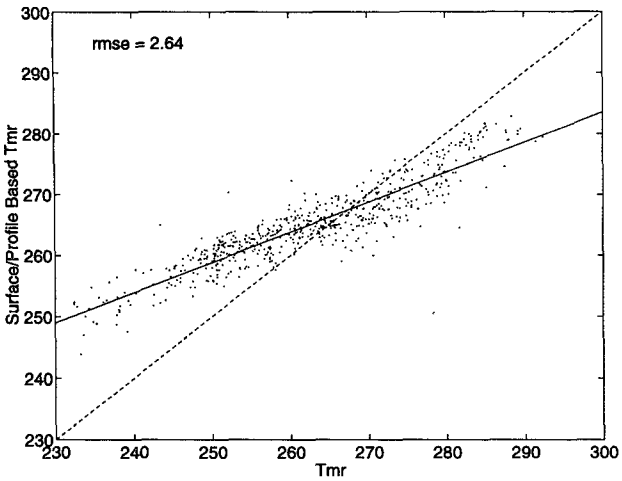

FIG. 8. Observed T_{mr} from radiosonde soundings vs T_{mr} calculated using a profile estimate after Robinson (1988).

FIG. 9. Gridpoint locations for the archive NGM B-grid model output.

those computed from the radiosonde measurements, a decided influence of the surface temperatures is seen (Fig. 8). This bias acts to shift predicted values of T_{mr} away from extremes. Consequently, the projected T_{mr} value can be seen to converge to a site-specific climatological mean value, with similar undesirable properties as described above. Despite the effort to relieve the WVR site on the dependency of outside data sources, we find that the best-fit line (rmse = 2.65) is not that of a one-to-one correspondence, but instead, a line with slope approximately 0.5. Thus, to take advantage of the improvements of this method, an individual site climatology must be developed to determine the linear model.

4. T_{mr} calculation using NWP model output

Here we introduce a new method of calculating T_{mr} that exploits the prior information content of NWP models. Output from the National Meteorological Center Nested Grid Model (NGM) is archived at the National Center for Atmospheric Research and was chosen for this study for its accessibility. The NGM archive dataset has a horizontal resolution of 190.5 km (Fig. 9) and contains fields of temperature and relative humidity at nine pressure levels (1000, 950, 900, 850, 800, 750, 700, 500, and 300 mb). The NGM output for 12-h forecasts (t + 12 h) is used to compute temperature and moisture profiles at all upper-air station locations within the model domain by interpolating the gridpoint data to the station location at each model level through bilinear interpolation. Here, T_{mr} is calculated from sounding profiles constructed at the station locations. The resulting values are then compared to values obtained from observed radiosonde data at the forecast time.

Values of T_{mr} obtained from the model forecast method described above show excellent agreement with those obtained from radiosonde soundings over the entire operational sounding network (Fig. 10), providing an rmse of 2.58 K ($\approx$1%). In contrast to the profile method above, we find that the values derived from the model output do fall along the line of one-to-one correspondence. Figure 11 displays the results of a 2-month operational use of NGM data to provide 12-h forecasts at individual sounding sites. Three locations: Nassau, Bahamas; Midland, Texas; and Caribou, Maine, representative of differing climatic regions, are used to illustrate the ability for this method to provide good predictions of the time variations as well as the overall seasonal and climatic tendencies.

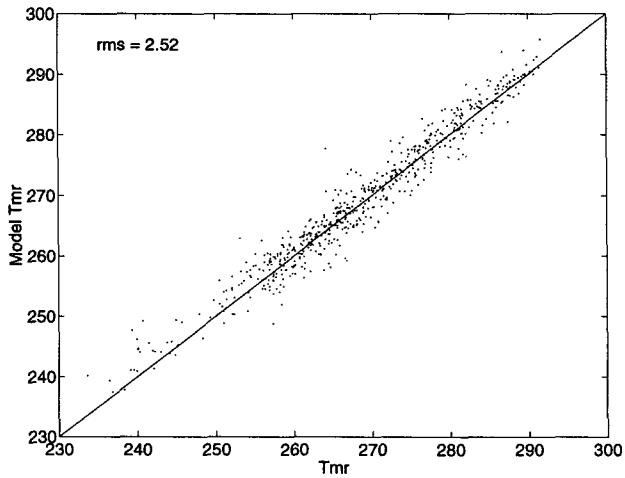

FIG. 10. Observed T_{mr} (31.4 GHz) from radiosonde soundings vs 12-h NGM model prediction.

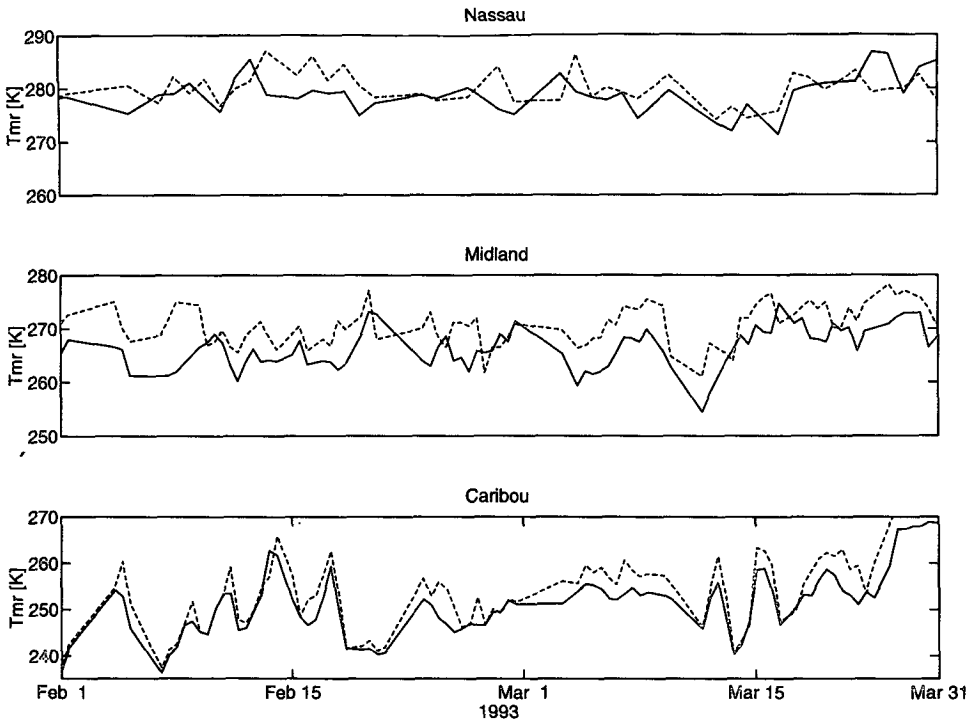

FIG. 11. Observed (solid lines) and predicted (dashed lines) values of T_{mr} (31.4 GHz) for 1 February–31 March 1993 at Nassau, Bahamas (top), Midland, Texas (middle), and Caribou, Maine (bottom). Predicted values are based on 12-h model forecast fields valid at the time of sounding.

The largest source of disagreement with the in situ soundings is apparently due to the lack of model levels in the planetary boundary layer in the archive dataset. In contrast, the radiosonde data can greatly contribute to the amount of water vapor in the lower levels of integration. It should be noted that while the archived NGM data used has a resolution of 190.5 km and nine vertical levels, operational NGM output currently has a resolution of approximately 90 km, with 16 vertical levels. Thus further improvement using this method should be expected as model data with greater resolution are applied. Another possible source of deviation can be found in the quality of radiosonde data transmitted from sounding locations. Since not all soundings used in the above comparison reported data to the 300-mb level, and no attempt was made to either remove or enhance these reports, it is possible that these observations result in a greater discrepancy than do more successful ascents. Since cloud layers are often very thin, the generally higher vertical resolution of radiosonde soundings is better able to resolve liquid water density in cloud layers as parameterized in (A4).

5. Conclusions

Improvement in WVR retrieval algorithms is critical to their successful application in atmospheric sciences and in Global Positioning System (GPS) and very long baseline interferometry (VLBI) geodesy. The use of NWP model output can greatly reduce the uncertainty of WVR measurements by improving the a priori knowledge of atmospheric conditions. Atmospheric water vapor is highly variable within the troposphere, especially in the vicinity of atmospheric disturbances such as storm systems and frontal zones where gradients in water vapor may be large, and the temporal and spatial resolution of radiosonde soundings may be inadequate to resolve variations on the storm scale. By using meteorological models, local weather conditions can be resolved on smaller scales than standard radiosonde soundings.

The improvement of the T_{mr} calculation using 12-h forecast output of the NGM model rather than climatological values or methods based on surface measurements yields a corresponding improvement of comparable magnitude in the retrieval of atmospheric opacity. Use of forecast model data relieves a WVR site of its dependency on local climatology or the necessity of a nearby sounding, allowing more accurate retrieval of observed conditions. Additionally, we find that the linear model given by (3) does not require a time-dependent $\gamma(t)$ when T_{mr} is calculated from the model. These results were obtained using an archived subset of the full NGM model output. Added horizontal and vertical resolution of model output should further improve these calculations.

Acknowledgments. This work has been supported by National Science Foundation Grant ATM-9207111. The authors wish to thank E. Westwater for his thorough review of this paper, as well as his knowledgeable suggestions for its improvements. The authors also would like to express their gratitude to the anonymous reviewers, whose comments and criticisms have been both helpful and insightful in preparing this paper.

APPENDIX

Computation of Optical Depth and Absorption Coefficients

In Eq. (2), τ can be expressed as the sum of that due to oxygen, water vapor, and liquid water. Thus,

$$\tau = \tau_{O_2} + \tau_v + \tau_l \qquad \text{(A1)}$$

and

$$\tau(s) = \int_{s'<s} \alpha(s')ds', \qquad \text{(A2)}$$

where s is the path distance of integration. Values for opacities are typically calculated using empirical fits to the observed frequency spectra (Waters 1976; Davis 1986; Elgered et al. 1991). These empirical fits, or line shape models are themselves limited to the individual experimental errors (Elgered et al. 1991). The opacities for the three components above are given by Davis (1986) as

$$\alpha_{O_2} = 2.6 \times 10^{-8} \frac{P\nu^2}{1013.25}\left(\frac{293}{T}\right)^3 \times \left[\frac{\Delta\nu_{O_2}}{(\nu-\nu_0)^2+(\Delta\nu_{O_2})^2} + \frac{\Delta\nu_{O_2}}{(\nu+\nu_0)^2+(\Delta\nu_{O_2})^2} + \frac{\Delta\nu_{O_2}}{\nu^2+(\Delta\nu_{O_2})^2}\right] (\text{cm}^{-1}) \qquad \text{(A3)}$$

$$\Delta\nu_{O_2} = 0.75\left(\frac{P}{1013.25}\right)\left(\frac{293}{T}\right)^{0.85}$$

$$\alpha_v = 3.43 \times 10^{-3} e^{-644/T}\nu^2\rho_v T^{-2.5} \times \left[\frac{\Delta\nu}{(\nu-\nu_0)^2+(\Delta\nu)^2} + \frac{\Delta\nu}{(\nu+\nu_0)^2+(\Delta\nu)^2}\right] + 2.55 \times 10^{-8}\rho_v\nu^2 T^{-1.5}\Delta\nu\ (\text{cm}^{-1})$$

$$\Delta\nu = 2.58 \times 10^{-3}\left(1 + 0.0147\frac{\rho_v T}{P}\right)\frac{P}{(T/318)^{0.625}}$$

$$\alpha_l = 10^{-6}\frac{\rho_l}{\lambda^2} e^{0.0281(291-T)}\ (\text{cm}^{-1}),$$

where ν (GHz) is the frequency of the signal, ρ_v (g m^{-3}) is the density of water vapor, ρ_l (g m^{-3}) is the liquid water density, and λ (cm) is the wavelength. Standard values for ν_0 are 60 GHz for oxygen and 22.235 GHz for water vapor. Values of 23.8 and 31.4 GHz were assumed for ν as typical WVR frequencies for this study.

To compute T_{mr}, the liquid water density must be estimated since it is not an observed quantity from sounding data, nor is it a standard output quantity in the model archive data. Westwater (1978) has shown that cloud liquid water is a limiting factor in water vapor retrievals, and must be included in the radiometer algorithms. A simple method for estimating ρ_l assumes clouds will exist at any altitude where the relative humidity is greater than or equal to 94% (Gary et al. 1985). Within the cloud layer the liquid water density at any height h is given as a function of the vapor density:

$$\rho_l(h) = 0.5[\rho_v(h_{base}) - \rho_v(h)], \qquad \text{(A4)}$$

where h_{base} is the altitude of the base of the cloud layer. To avoid unrealistically thick clouds, a maximum value of 2.0 g m^{-3} is imposed. Robinson (1988) has suggested that T_{mr} for microwaves is not particularly sensitive to the exact formulation used for liquid water. Figure A1 shows the contribution of liquid water to T_{mr} in over 600 soundings. From Fig. A1 it is clear that the overall contribution of liquid water is generally less than a few percent, and the variation in the resultant T_{mr} calculation due to specific cloud models may not be large. Decker et al. (1978) employed a similar parameterization scheme for three cloud models, based on a 95% relative humidity threshold for cloud presence and a constant liquid density with height. The value of cloud density was determined by the cloud thickness and one of three profiles based on observed conditions. Davis (1986) reviewed the three possible cloud water profiles used by Decker et al. (1978) and reported that the effect of the different cloud models produced a 0.1-K difference in T_{mr}.

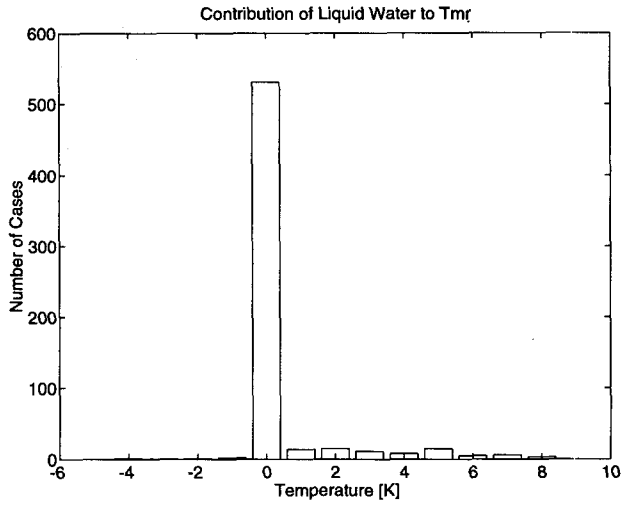

FIG. A1. Contribution of liquid water to T_{mr} for 600 soundings within the NGM model domain.

The primary differences in the two models discussed above is that Decker et al. (1978) assumes a constant distribution of liquid water density with a maximum value of 0.8 g m^{-3}, whereas Gary et al. (1985) uses a variable distribution given by (A4) with a maximum of 2.0 g m^{-3}. The maximum value of 2.0 g m^{-3} would be more representative in cumulus cloud cases than 0.8 g m^{-3} and would consequently result in a larger contribution to T_{mr}. We have used (A4) throughout the calculations in this paper.

The above discussion on the difficulty in parameterizing cloud liquid water content from a sounding or climatology emphasizes the utility of NWP models in this area. At present, cloud liquid water is not a standard output field in operational models, but it is included in the computations. In the future, it may be possible to incorporate this data directly in the T_{mr} calculation.

REFERENCES

Askne, J., and H. Nordius, 1987: Estimation of tropospheric delay for microwaves from surface weather data. *Radio Sci.*, **22,** 379–386.

Bevis, M., S. Businger, T. Herring, R. A. Anthes, C. Rocken, and R. H. Ware, 1992: Remote sensing of atmospheric water vapor using the global positioning system. *J. Geophys. Res.*, **97,** 15 787–15 801.

Davis, J. L., 1986: Atmospheric propagation effects on radio interferometry. Scientific Report No. 1, AFGL-TR-86-0243, Air Force Geophysics Laboratory, 276 pp.

Decker, M. T., E. R. Westwater, and F. O. Guiraud, 1978: Experimental evaluation of ground-based microwave radiometric sensing of atmospheric temperature and water vapor profiles. *J. Appl. Meteor.*, **17,** 1788–1795.

Elgered, G., J. L. Davis, T. A. Herring, and I. I. Shapiro, 1991: Geodesy by radio interferometry: Water vapor radiometry for estimation on the wet delay. *J. Geophys. Res.*, **96,** 6541–6555.

Gary, B. L., S. J. Keihm, and M. A. Janssen, 1985: Optimum strategies and performances for the remote sensing of path-delay using ground-based microwave radiometers. *IEEE Trans. Geosci. Remote Sens.*, **23,** 479–484.

Hogg, D. C., F. O. Guiraud, and W. B. Sweezy, 1981: The short-term temporal spectrum of precipitable water vapor. *Science,* **213,** 1112–1113.

Liou, K., 1980: *An Introduction to Atmospheric Radiation.* Academic Press, 392 pp.

Resch, G. M., 1984: Water vapor radiometry in geodetic applications. *Geodetic Refraction,* F. K. Brunner, Ed., Springer-Verlag, 213 pp.

——, M. C. Chavez, N. I. Yamane, and R. C. Chandlee, 1985: Water vapor radiometry research and development phase final report. Jet Propulsion Laboratory Publication 85-14, 96 pp.

Robinson, S. E., 1988: The profile algorithm for microwave delay estimation from water vapor radiometer data. *Radio Sci.,* **23,** 401–408.

Rocken, C., 1988: The Global Positioning System: A new tool for tectonic studies. Ph.D. thesis, University of Colorado, 298 pp.

——, J. M. Johnson, R. E. Neilan, M. Cerezo, J. R. Jordan, M. J. Falls, L. D. Nelson, R. H. Ware, and M. Hayes, 1991: The measurement of atmospheric water vapor radiometer comparison and spatial variations. *IEEE Trans. Geosci. Remote Sens.,* **29,** 3–8.

U.S. Standard Atmosphere Supplements, 1966: Environmental Science Services Administration. NASA/USAF. U.S. Government Printing Office, Washington, DC, 289 pp.

Waters, J. W., 1976: Absorption and emission by atmospheric gases. *Methods of Experimental Physics: Astrophys,* M. L. Meeks, Ed., Academic Press, 142–175.

Westwater, E. R., 1978: The accuracy of water vapor and cloud liquid determinations by dual-frequency ground based microwave radiometry. *Radio Sci.,* **13,** 677–685.

Wu, S. C., 1979: Optimum frequencies of a passive radiometer for tropospheric path-length correction. *IEEE Trans. Antennas Propag.,* **27,** 233–239.